

Interactions in planar metamaterials and their use for active tuning

I. Brener^{1,2}, A. Gabbay^{1,2}, X. Miao^{1,2}, B.S. Passmore¹, J. Reno^{1,2}, J.R. Wendt¹, A. Gin^{1,2}, M.C. Wanke¹, M.B. Sinclair¹, E.A. Shaner¹, D.J. Shelton³, J.C. Ginn^{1,2}, D.W. Peters¹, G.D. Boreman³, S. Vangala⁴, W. Goodhue⁴

¹ Sandia National Laboratories, P.O. Box 5800, Albuquerque, NM 87185

² Center for Integrated Nanotechnologies, P.O. Box 5800, Albuquerque, NM 87185

³ CREOL, University of Central Florida, 4000 Central Florida Blvd, Orlando, FL 32816, USA

⁴ Department of Physics and Applied Physics, University of Massachusetts Lowell, Lowell, MA 01854, USA

Abstract

We explore strong coupling between metamaterial resonators and different types of absorbers placed in proximity to these resonators. Very clear anticrossing behaviour and level splitting is observed when IR phonons interact with metamaterials. More complex dipole transitions can be designed using semiconductor bandgap engineering. We show experimentally the coupling between metamaterial resonances and intersubband transitions and highly doped layers in semiconductor heterostructures and discuss this mechanism for electrical tuning of metamaterials throughout the optical infrared spectral region.

1. Introduction

Planar metamaterials (or “metafilms”) offer a promising platform for new types of active optical devices. Resonances in these metamaterial structures can be scaled by geometry and their spectral response is exquisitely sensitive to the local dielectric environment which can be changed using a number of tunable dielectrics¹⁻³. Arrays of metamaterial resonators have already been used as amplitude and phase modulators at terahertz frequencies.^{4,5} In this paper we further explore the interaction between metamaterial resonators and various dipole resonances and discuss applications for electrical tuning of metamaterials.

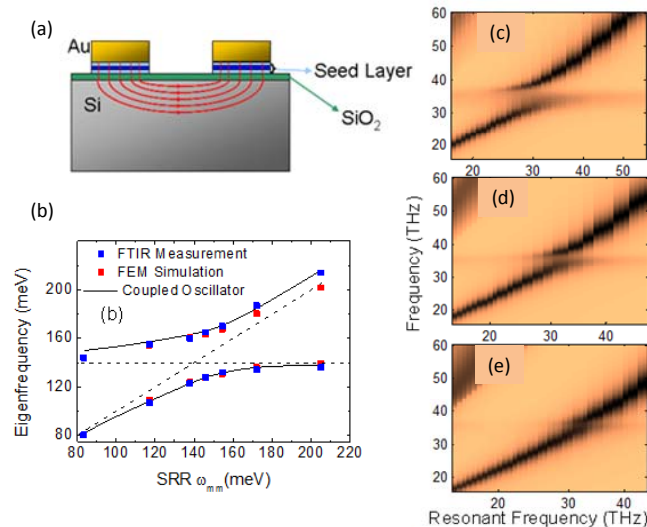


Fig. 1: (a) Schematic cross section showing thin film interface between metallic SRR elements and Si wafer including a thin SiO₂ layer. (b) the measured resonant frequencies of the coupled modes compared to the analytical model for two coupled oscillators. (c-e) Normal mode splitting simulated by FDTD as the SiO₂ layer is displaced from the SRR metamaterial elements: (c) SiO₂ in contact, (d) SiO₂ depth of 50nm, (e) SiO₂ depth=125nm.

2. Strong interaction between metamaterials and infrared phonons.

Infrared phonons in dielectrics placed in proximity with metamaterial resonators can couple strongly, leading to normal mode splitting similar to vacuum-Rabi splitting that occurs with optical emitters coupled to microcavities. The amount of coupling can be altered through the design of the metamaterial resonators, the proximity of the dielectric layer to the resonator, the dielectric film thickness, and the amount of field overlap with the dielectric layer.⁶ An example is shown in Fig. 1 where split ring resonators (SRR) were fabricated on a Si substrate with a 10nm Silicon oxide film. A schematic diagram is shown in Fig. 1(a); as the SRR dimensions are scaled and the fundamental resonance is swept through the IR Si-O phonon band, a clear anticrossing is observed, indicative of strong coupling (Fig. 1(b)). The coupling strength can be further controlled by varying the depth of this dielectric layer as is shown in modeling results in Fig. 1(c).

2. Interaction with doped layers and tuning in the thermal infrared.

The interaction of planar metamaterial resonators with electron sheets directly underneath the metal traces has been exploited as an active tuning mechanism for Terahertz beams.⁷ Scaling this approach to higher infrared frequencies poses serious challenges as the plasma frequency of doped semiconductors does not scale easily to these frequencies (this requires high mobility and/or extremely high doping densities). Instead of resonance damping through the interaction with lossy semiconductor doped layers, a more attractive mechanism for metamaterials tuning in the infrared is to use doped semiconductors that show significant changes in their permittivity with electron density. An example of this approach is shown in Fig. 2 where SRR arrays were fabricated on top of doped InSb layers.⁸ Electrons in n-doped InSb have among the highest mobilities of all semiconductors and thus plasma frequencies in the mid IR are within reach. As the electron density is varied (statically in this case but feasible with an active gate), the SRR resonance shifts in wavelength by more than 20%, and without significant damping.

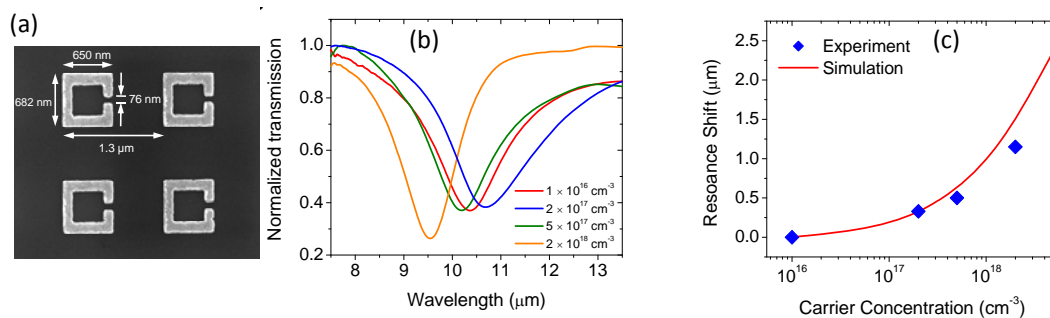


Fig. 2: (a) Scanning electron microscopic image of the SRRs fabricated on InSb substrate. (b) The transmission spectra for the metamaterial with SRRs fabricated on the InSb substrate with doping levels of 2×10^{16} cm⁻³, 2×10^{17} cm⁻³, 5×10^{17} cm⁻³, and 2×10^{18} cm⁻³, respectively. The polarization direction of the incident light is parallel to the SRR gap. (c) The resonance shift when the carrier concentration is increased from the intrinsic level. The red curve shows the results from finite element simulation. The blue dots are the experimentally measured values.

3. Interaction with infrared intersubband transitions using bandgap engineered heterostructures.

Another tuning mechanism that we are currently exploring is the interaction of metamaterial resonances with intersubband transitions (IST) in semiconductor heterostructures. The major advantage of ISTs is the wide scalability in wavelength response that can be obtained through QW structural parameters such as the doping level, energy spacing between subbands and the use of different material systems. An example is shown in Fig. 3: arrays of SRRs and control square loops were fabricated on

top of a semiconductor heterostructure consisting of two coupled QWs as the basic unit cell. The quantum well structure was grown by molecular beam epitaxy (MBE) and consists of 30 repetitions of a unit cell comprised of a coupled quantum well (QW) structure 15/5.75/1.13/2.5/15 nm thick layers of ($\text{Al}_{0.5}\text{Ga}_{0.5}\text{As}/\text{GaAs}$), followed by a Si δ -doped layer. The electron density within each coupled QW structure is about $2 \times 10^{11} \text{cm}^{-2}$. The selection rules for this type of engineered transition are such that the optical field needs to have TM components, namely, inside the plane of the QWs. Even upon normal incidence in a TE geometry, a significant fraction of TM light is provided through the fringing fields of the SRRs. We scale the SRR geometry and sweep it through the IST transition designed at $\lambda \sim 10 \mu\text{m}$. Significant interaction can be observed for the polarization parallel to the gap (Figs. 3(c-e)), as evidenced by the broadening of the resonance in comparison with the same SRR arrays fabricated on a control undoped GaAs wafer. These effects can now be coupled with electrical tuning of the sub-band levels in order to electrically tune metamaterial resonances and this will be discussed in the talk.

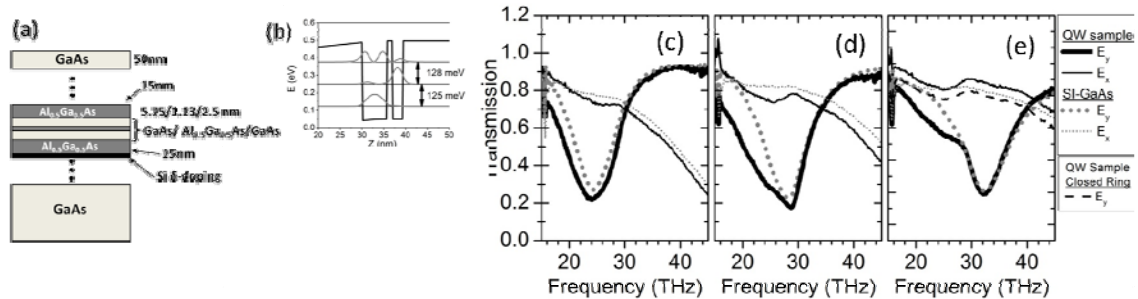


Fig. 3: (a) - The layer sequence of the QW sample. (b) An energy band diagram of two asymmetric coupled QWs. The subbands and their corresponding wavefunctions (modulus) are shown as well. (c-e) Transmission spectra for three different SRR arrays, which were scaled (length, linewidth, gap size and periodicity) to resonate at different frequencies. The legend indicates the polarization of the incident light for each transmission line and the substrate beneath the SRRs.

This work was performed, in part, at the Center for Integrated Nanotechnologies, a U.S. Department of Energy, Office of Basic Energy Sciences user facility and is supported by the Laboratory Directed Research and Development program at Sandia National Laboratories. Partial funding provided by the Energy Frontier Research Center for Solid State Lighting Science and DARPA/MTO's Casimir Effect Enhancement program under DOE/NNSA Contract DE-AC52-06NA25396. Sandia National Laboratories is a multiprogram laboratory operated by Sandia Corporation, a Lockheed-Martin Co., for the U. S. Department of Energy under Contract No. DE-AC04-94AL85000.

References

1. H.-T. Chen, W. J. Padilla, J. M. O. Zide, et al., *Nature* **444** (7119), 597-600 (2006).
2. M. J. Dicken, K. Aydin, I. M. Pryce, et al., *Optics Express* **17**, 18330-18339 (2009).
3. T. Driscoll, S. Palit, M. M. Qazilbash, et al., *Applied Physics Letters* **93** (2), 024101 (2008).
4. H.-T. Chen, W. J. Padilla, M. J. Cich, et al., *Nat Photon* **3** (3), 148-151 (2009).
5. X. Peralta, I. Brener, W. Padilla, et al., *Metamaterials* (2010).
6. D. J. Shelton, D. W. Peters, M. B. Sinclair, et al., *Optics Express* **18** (2), 1085-1090 (2010).
7. H. Chen, J. O'Hara, A. Azad, et al., *Nature Photonics* **2** (5), 295-298 (2008).
8. X. Miao, B. Passmore, A. Gin, et al., *Appl. Phys. Lett.* **96**, 101111 (2010).